ORIGINAL RESEARCH

Focused Energy, A New Approach Towards Inertial Fusion Energy

T. Ditmire[1,2] · M. Roth[1,2] · P. K. Patel[1,2] · D. Callahan[1,2] · G. Cheriaux[1,2] · P. Gibbon[1,2] · D. Hammond[1,2] ·
A. Hannasch[1,2] · L. C. Jarrott[1,2] · G. Schaumann[1,2] · W. Theobald[1,2] · C. Therrot[1,2] · O. Turianska[1,2] ·
X. Vaisseau[1,2] · F. Wasser[1,2] · S. Zähter[1,2] · M. Zimmer[1,2] · W. Goldstein[1,2]

Abstract

Focused Energy is a new startup company with the goal of developing laser-driven inertial fusion energy for electrical power production. The company combines the results from decades of fundamental research in inertial confinement fusion at universities and national laboratories with the flexibility and the speed of a startup company. Focused Energy has chosen the direct-drive, proton fast ignition approach to reach ignition, burn and high gain as the most promising approach. Located in Austin/US and Darmstadt/Germany, supported by the science community and private investment Focused Energy is paving the way to inertial fusion energy combining the best skill set and state-of-the-art technology from both sides of the Atlantic Ocean. In this paper we discuss the details and reasoning for the approach and the technical directions we have chosen. We will outline our roadmap for getting to a fusion pilot plant in the mid to late 2030s.

Keywords Fusion · Laser · Fast ignition · Proton fast ignition · Inertial fusion

Introduction

Fusion energy has been among the most challenging problems addressed by the science community since the 1950's. While fusion research has been largely academic and programmatic within large national laboratories, recent progress has now made it plausible to commercialize fusion energy within less than two decades. This has led to an exuberant establishment of private industry start-ups devoted to realizing this commercialization. The essence of the challenge is well known. First, a burning plasma must be achieved, which mandates sufficiently high temperature, one in which the self-heating of the plasma by the fusion products overcomes the energy losses. However, hot plasma is subject to several cooling mechanisms: as it

✉ T. Ditmire
todd.ditmire@focused-energy.world

✉ M. Roth
markus.roth@focused-energy.world

1   Focused Energy Inc, 11525-B Stonehollow Drive, Austin, TX 78758, USA

2   Focused Energy GmbH, Im Tiefen See 45, 64293 Darmstadt, Germany

expands, it will cool adiabatically. In addition, energy loss by bremsstrahlung radiation is important, particularly if the fusion fuel is composed of ions of higher atomic number (bremsstrahlung scales as Z^2, where Z is the ionization degree) or if there are high Z impurities in the plasma. Hence, the plasma must be kept at a high temperature and needs to be confined so that the energy gain from fusion reactions replenishes the energy that is lost, and the plasma can be used for energy production.

The metric to overcoming this balance is quantified by the well-known Lawson criterion [1], which is given for deuterium tritium (DT) fusion plasmas by the equation:

$$n\tau > k_B T / (<\sigma v> E_{fus}) \approx 10^{14} s/cm^3,$$

where n is the plasma density, τ is the confinement time, $k_B T$ is the thermal energy with k_B the Boltzmann constant and T the fuel temperature, $<\sigma v>$ is the probability of a fusion reaction averaged over a Maxwellian distribution of velocities of the particles, and E_{fus} is the energy released in the fusion reaction. Until recently this metric has not been reached in controlled laboratory conditions. However, in December 2022 this was exceeded for the first time [2]. Breaking this threshold is one of the principal motivations for attempting now to commercialize fusion energy. There have been traditionally two distinct approaches to

controlled fusion, magnetic confinement fusion (MCF) [3] and inertial confinement fusion (ICF) [4–6], although there are many variations of both concepts and several other exotic approaches. MCF has not yet reached break-even. The Joint European Torus (JET) facility reported recently that they broke their previous yield record by $> 2 \times$ generating 59 MJ over a 5 s duration with an average power of $\sim$ 11 MW. But the plasma heating power was upgraded to almost 40 MW to do so resulting in a gain or Q value of 0.33 compared to Q = 0.67 in the 1997 record shot [7–9], It is the ICF approach, which led to scientific breakeven from the now well-known result on the National Ignition Facility (NIF)[2, 10] at Lawrence Livermore National Laboratory and it is this approach, which we are exploiting as a path to commercialize fusion energy.

Inertial Confinement Fusion

To match the Lawson criterion, hot plasma can be either confined at a low density (10^{14}/cm^3) for a long time ($>$ s) (MCF) or for a very high density (10^{26}/cm^3) for a very short time ($>$ ps) (ICF). This separates the two main approaches in fusion energy research. The different stages of ICF are illustrated in Fig. 1 and the concept is well discussed in Refs. [4, 5]. ICF places itself at the high-density end of the Lawson criterion. The underlying idea is to compress a spherical target to roughly a thousand times of solid density. The confinement time $\tau = R_f/c_s$ is governed by the size of the assembled fuel (R_f) divided by the maximum speed the fuel can expand, which is determined by the sound velocity of the plasma: $c_s = (2k_BT/m_i)^{1/2}$, where m_i is the mass of the ion. There is a practical upper limit to the compressed fuel mass that can be employed in a fusion reactor, since released energy above a few GJ (1 GJ $\sim$ 240 kg TNT equivalent) cannot be handled mechanically by any realistic reactor vessel. The way the fuel is assembled and compressed is by using a spherical rocket effect. A small capsule (mm size) is composed of a thin shell of an outer ablator layer and a solid (cryogenic) DT fusion fuel layer. The outer part of the capsule is promptly irradiated with energy (lasers, x-rays, heavy ions). This ablating plasma forms the spherical rocket engine, where the ablation pressure drives the inner part of the capsule inwards forming the dense fusion fuel close to the center.

The most widely pursued ICF approach, and the one that led to ignition on the NIF, is the so-called central hot-spot ignition approach [5, 9]. The capsule is compressed in such a way that the entropy of the dense shell is kept at a minimum so that the incoming fusion fuel shell can be compressed to high density. The high-density shell encapsulates a lower density fuel plasma at the center, which is formed from the initial gas in the capsule and from ablated material of the inside wall of the shell. When the implosion reaches stagnation, the kinetic energy of the incoming shell is transferred into thermal energy in the hot-spot fuel plasma and raises its temperature to ignition conditions. As the fuel starts burning in the center, alpha particles produced as one of the products of each fusion reaction deposit their energy in the hot spot, which launches a spherical burn wave that propagates through the cold fuel shell faster than the main part of the fuel can expand at the local sound velocity.

In conventional hot-spot ignition, only a small amount of the fuel is brought to ignition conditions. The
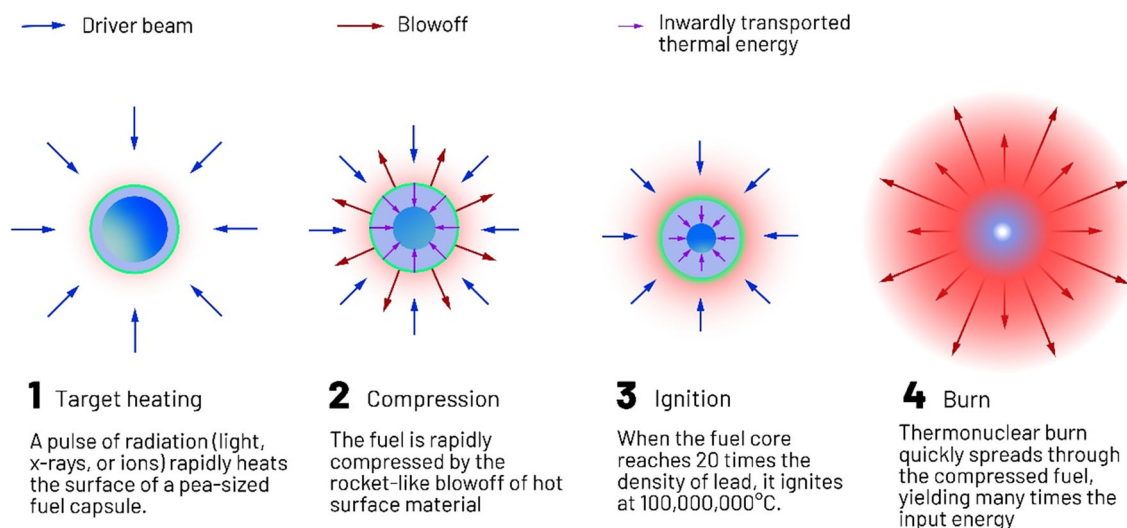

1 Target heating
A pulse of radiation (light, x-rays, or ions) rapidly heats the surface of a pea-sized fuel capsule.

2 Compression
The fuel is rapidly compressed by the rocket-like blowoff of hot surface material

3 Ignition
When the fuel core reaches 20 times the density of lead, it ignites at 100,000,000°C.

4 Burn
Thermonuclear burn quickly spreads through the compressed fuel, yielding many times the input energy

Fig. 1 Inertial confinement fusion stages with **a** irradiation of the outer layer, **b** ablation of the outer material and implosion of the payload, **c** central ignition, and **d** burn and explosion

temperature is provided by thermalization of the kinetic energy of the cold, dense fuel shell compressing and heating the low-density part of the fuel in the center. To achieve ignition it is vital to provide a) a high shell velocity (> 350 km/s for DT), b) a close to perfect spherical implosion, c) negligible contamination with any high-Z material as radiation losses scale with Z^2, and d) an areal density, $(\rho R)_{hot}$, of the hot spot that matches the range of the alpha particles to deposit the fusion energy in that volume. $(\rho R)_{hot} \equiv \int_0^{R_{hot}} \rho dr$, where R_{hot} is the hot spot radius, ρ is the mass density, and r is the radius. If these conditions are fulfilled the plasma in the hot spot undergoes a bootstrapping in energy and temperature increases where the fusion energy diffuses into the cold fuel as a supersonic burn wave that consumes a certain fraction of the surrounding initially cold fusion fuel, depending on the total areal density of the fuel. The yield of the igniting target only depends on the amount of the assembled fuel mass and its total areal density, which are limited by the amount of available drive laser energy and, ultimately, by the maximum yield that can be handled by the reactor vessel. Figure 2 illustrates a typical hot spot ignition target (a) for direct laser irradiation with the power history of the laser and (b) the time history of the radial propagation of the various shocks and the trajectory of the compressed shell, reaching ignition at roughly 11 ns after the ablating compression pulses have begun [11].

Direct and Indirect Drive

The goal of achieving a symmetrical implosion has been approached by two different schemes: indirect drive and direct drive, illustrated schematically in Fig. 3. In indirect drive [5], the fuel capsule is embedded in a high-Z container (a hohlraum), whose inside surface is heated by the primary laser driver. The laser beams enter the hohlraum through laser entrance holes and irradiate the inner surface of the container. The resulting homogeneous, soft x-ray radiation immerses the fusion capsule at the center of the hohlraum and the deposited x-ray energy then ablates the outer surface of the capsule. In the direct-drive approach [11], a homogeneous radiation field on the outside of the capsule is established by using numerous laser beams with overlapping focal spots. Both concepts have been pursued in the US ICF program, with the National Ignition Facility (NIF) [12, 13] at Lawrence Livermore National Laboratory (LLNL) leading the indirect-drive development and the OMEGA laser [14] at the Laboratory for Laser Energetics (LLE) at the University of Rochester leading the direct-drive approach.

One drawback for the commercialization of the indirect-drive approach in an inertial fusion energy (IFE) program is the inefficiency of the hohlraum. Typically, only 10–15% of the energy ends up being absorbed by the capsule. This is because roughly 50% of the laser energy ends up in the hohlraum wall and about 30–35% is radiated out of the laser entrance holes (the balance of about 5% is used to heat up materials inside the hohlraum) [15]. There can also be additional laser-plasma-instabilities [15, 16], which backscatter laser light back out of the hohlraum–in current low hohlraum gasfill designs, the losses due to backscatter tend to be small [17]. This inefficiency makes it difficult to achieve high gain that is needed for IFE. In comparison, the efficiency for direct drive is about a factor of 5 higher [18].

Hot spot ignition

In ICF, ignition and propagating burn occurs when there is a sufficient temperature (5–10 keV) reached within a mass
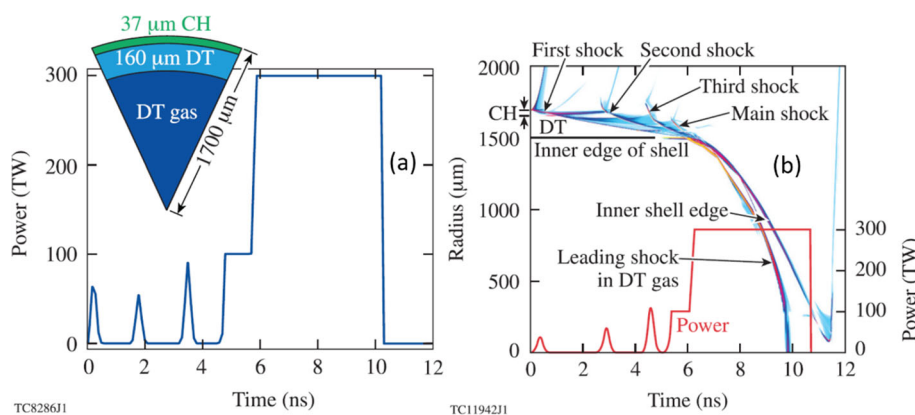

Fig. 2 Ignition design of a hot spot ICF target with **a** target and laser pulse shape for direct-drive irradiation and **b** contour plot in the (radius, time) plane of the inverse pressure scale length showing the trajectories of the various shocks and the in-flight shell trajectory. A thin payload is required to reach the high inflight velocity. Once the kinetic energy is thermalized at stagnation and ignition is reached, a supersonic burn wave propagates outwards. Figure reproduced from Ref. [11], American Institute of Physics

**Fig. 3** Indirect drive **a** and direct-drive **b** ICF approach
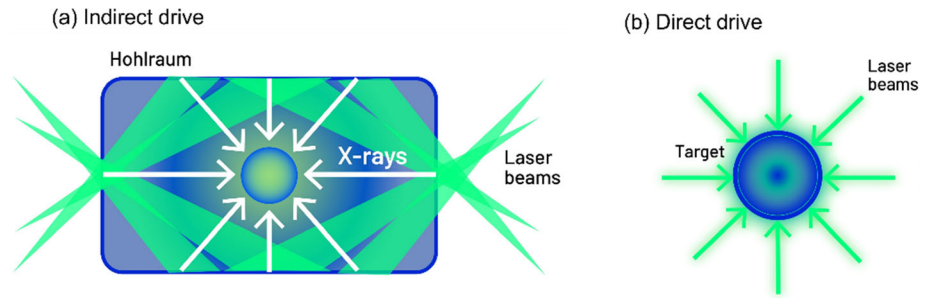
of DT fuel characterized by an areal density greater than an alpha particle range $(\rho r)_\alpha > 0.3$ g cm^{-2} [4, 5, 19]. The necessary conditions are achieved by an appropriate balance between the energy gain mechanisms and the energy loss mechanisms. As it would be a waste of energy to heat the entire fuel to ignition temperatures only a part in the center of the compressed fuel is brought up to sufficiently high temperatures. To save energy, the main part of the fuel is kept at the lowest possible temperature as any increase in pressure of the cold fuel must be compensated by additional driver energy during compression. Indirect drive hot-spot ignition has been extensively explored since 2009 with the commissioning of the NIF. Much knowledge has been gained in the last 12 years [9, 20–23] and NIF has recently demonstrated a yield of more than 3100 kJ of fusion energy with a gain of 1.5 [10].

While these are encouraging results, showing the progress in understanding of compression and heating, the hot-spot conditions (temperature, pressure, and areal density) still must be improved. For this, the crucial, underlying challenge is that with one driver to compress and heat

simultaneously, there are four requirements that must be met at the same time, which are illustrated schematically in Fig. 4:

(1) The fuel must be compressed to a mass density of about 500 g/cm^3 and total areal density exceeding 1 g/cm^2. To do that using limited laser energy there must be no significant rise of the temperature in the cold fuel shell to avoid additional pressure increase in the dense shell. The extent to which that happens is characterized by the adiabat parameter α, which is defined as the ratio of plasma pressure inside the dense shell to the pressure of a Fermi-degenerate plasma.

(2) The shell velocity must reach at least 350 km/s to have enough kinetic energy to heat the low density hot-spot plasma to a temperature of > 5 keV upon stagnation and thermalization. To reach that velocity in less than 20 ns, an acceleration of 1.75×10^{12} g is required.

(3) The fuel capsule is first accelerated inwards and then deaccelerated when approaching stagnation, which

Fig. 4 The four principal challenges for successful central hot spot ignition. All must be met simultaneously
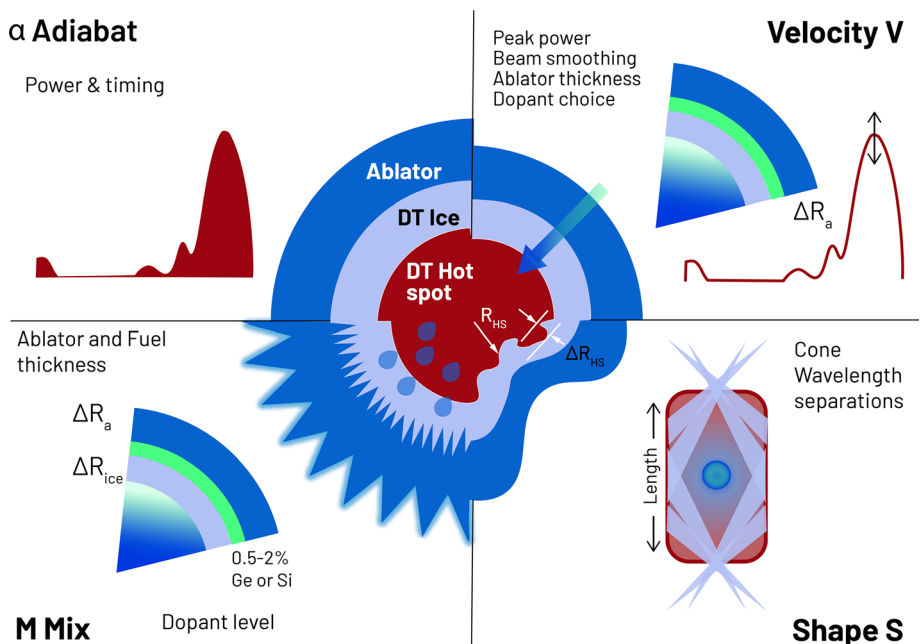
are both hydrodynamic unstable regimes. The interface between a heavy fluid and a light fluid in an accelerating field pointing toward the light fluid is Rayleigh–Taylor unstable.[24, 25] A small perturbation grows exponentially in time, $\sim e^{\gamma t}$, at a certain growth rate γ determined by the perturbation wave number, the ablation velocity, the acceleration, and the Attwood number [26–28]. This poses a significant trade-off with requirement 2, which requires a thin shell with high velocity for hot-spot ignition, which is more hydrodynamically instable than a thick shell imploding with a low velocity. If the shell breaks up from hydrodynamic instability growth, the cold outer fuel mixes with the high temperature hot spot region, so that ignition becomes impossible. Both indirect- and direct-drive experiments on NIF and OMEGA have struggled with underperformance at low adiabat [29–32]. While the physics is not fully understood, the main hypothesis is that low adiabat hot-spot ignition implosions are more susceptible to hydro-instability growth and mix.

(4) The coalescence of all the incoming fuel to an ideal hot spot demands a nearly perfectly round shape, which might be affected by non-uniformities in the driving radiation field [21, 33, 34].

The Focused Energy Ignition Concept

Controlled fusion in the laboratory is difficult; no one has demonstrated controlled fusion burn in a laboratory with a scheme ready for energy production. However, based on decades of research by the community, we have developed a basic design for a successful ignition target for fusion energy commercialization that is based on multiple, international studies [35–38]. Recently, a comparison of those studies suggests that there is a common focal point in the parameter space that we can attack. Essentially our approach is a result of decisions between several ways of achieving compression and heating.

Fast Ignition

An alternative is to perform the heating not through the compression but to separate it in a subsequent step by means of inputting additional energy into the pre-compressed fuel and creating a hot spot in that manner, a process known as the fast ignition [39] (FI) approach. This idea is schematically illustrated in Fig. 5. This path for a successful IFE commercialization separates the compression of the fuel and the heating of the required hot spot in a
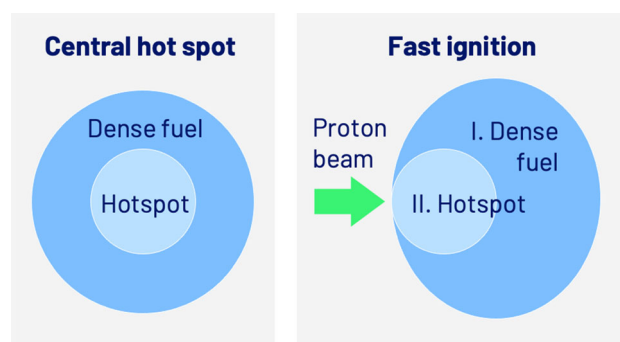

Fig. 5 Basic concepts of the central hot-spot (left) and the fast ignition (right) approaches. Fast ignition separates the compression from the ignition phase by adding a high intensity charged particle beam to ignite the fuel in a small volume on the left side of the dense fuel assembly

direct drive configuration. This is an approach, which has become possible in the past two decades through developments in new laser technologies and a better understanding of laser acceleration of particles. FI was proposed to increase the gain, reduce the laser energy, and relax the symmetry requirements for compression, primarily in direct drive. FI has being extensively studied by many groups worldwide [16, 17, 35, 37, 40–49]. It circumvents the roadblocks of conventional hot spot ignition and offers a higher energy gain for a given drive energy. This results in a smaller facility and the potential use of advanced fusion fuels that might offer enhanced reactor lifetime and less activation.

The idea behind fast ignition is to compress fuel first to high densities and then to heat a small volume in the dense fuel to ignition temperatures. The heated region has to provide the start of a self-sustaining burn wave into the surrounding fuel and thus has to reach the same $(\rho r)_{\alpha-} > \sim 0.3$ g cm^{-2} conditions as in the conventional ignition scheme. There is a tradeoff between required compression of the fuel and the required energy to heat the hot spot by an external source. The higher the density, the smaller the hot spot, the lower the required ignition energy, but the shorter the time window for delivering the ignition energy. Extensive studies have been made on this scheme numerically and benchmarked by experiments [35]. A common finding is that there is a "sweet spot" for the balance between compression and ignition energy for densities around 500–800 g/cm^3, which requires between 10 and 20 kJ of energy delivered to the hot spot in a period of 10 to 35 ps. Such theoretical studies are reported in Ref. [43, 50], showing in Fig. 6 a minimum in required ignition laser energy as a function of the density of the pre-compressed fuel.

The energy to heat the hot spot must be delivered to the dense part of the fuel. The laser is not able to reach that
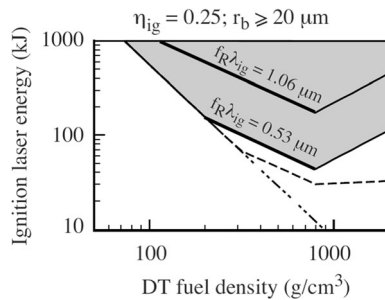
Fig. 6 Ignition laser energy for electron fast ignition as a function of the density of the pre-compressed fuel. A hot spot radius of 20 μm and an ignition laser beam energy coupling efficiency of 25% are assumed for different values of $f_R \lambda_{ig}$ (particle range parameter times laser wavelength). The dashed curve assumes a particle range that is independent of the beam intensity and shorter than 1.2 g/cm^2; the dotted-dashed line is the ignition scaling law that assumes optimal particle range and optimal beam radius. Figure reproduced from Ref. [43], American Institute of Physics

region as it is stopped at the critical density n_c, roughly one percent of solid density. This stops the laser at a surface well outside of the region of highly compressed fuel, prohibiting the laser heating the hot spot directly by classical collisional absorption. The deposited laser energy must be transported to the dense fuel at 1000 times solid density. The initial proposal and much of the research on the fast ignition approach for the past two decades focused on laser-generated electron beams [38, 39, 43, 45, 47, 48]. The biggest challenge to use electrons is the fact that their trajectories are easily bent by collisions and by self-generated electromagnetic fields inside the plasma that significantly degrades the coupled energy into the high-density fuel [47].

Our approach to FI was triggered by the discovery of intense, short, energetic, directed beams of protons off the rear surface of solid foil targets irradiated by ultra-intense lasers [51–58]. The ultra-intense laser generates fast electrons that propagate through a thin foil setting up space charge fields, which transfer energy from the electrons to the protons. With the discovery of intense, short ion bursts with excellent beam quality, we proposed the idea of using those beams for FI [59], the so-called proton fast ignition (PFI) approach. Using protons instead of electrons to ignite the fuel has several advantages. Protons penetrate deep into a target to reach the high-density region, where the hot spot is to be formed. Protons maximize the energy deposition at the end of their range to heat a more localized volume (via their Bragg peak). The basic idea, illustrated in Fig. 7, is to use multiple, short pulse lasers irradiating a thin foil that is mounted inside a cone structure to generate the igniting proton pulse. The protons are accelerated off the rear surface of the foil and, due to the curved shape of the foil are focused into the compressed fuel [60–62]. The higher mass makes them less likely to be subject of instabilities, which

provides excellent focusing. Furthermore, the pulse duration is short, and the particle numbers are high.

The PFI scheme we are pursuing is to fabricate targets composed of a capsule of cryogenic DT fuel (of 1 −2 mm diameter) and a high Z cone is inserted. The capsule is compressed by direct drive. As Fig. 7 illustrates, after compression, a thin (μm thick) foil in the shape of a hemisphere inside the cone is irradiated by picosecond pulses (in our scheme a 3 ps pulses with total energy of ∼ 150 kJ). This generates a focused proton beam which will form the hot spot.

In a fast ignition target the shell is thicker than in conventional ignition, so the target is less sensitive to hydrodynamic instabilities. The lower in-flight velocity (no thermalization of the kinetic energy is required) reduces the growth rate of instabilities and the larger amount of dense fuel offers a higher yield, which is required for commercial IFE. FE uses the direct drive approach, omitting the hohlraum and associated losses in efficiency. Modern laser pulse shaping techniques combined with an increase in laser bandwidth are a promising path forward in the suppression of laser-plasma-instabilities (LPI) [15] and are opening the possibility to apply 527 nm rather than 351 nm wavelength light for target compression. FE is planning to use the second harmonic light of the 1 μm wavelength light from a Nd:glass laser (instead of the third harmonic light) for compression (discussed in more detail below). This allows for a smaller, more cost effective and more efficient laser facility that reduces the wear and tear on the optics in high repetition rate operation.

The target uses a cone-in-shell geometry. The laser-driven proton beam is poly-energetic and needs to be focused to around 30–40 μm. The ion beam must be produced close to the fuel, as scattering and velocity dispersion will enlarge the irradiated area and pulse duration, requiring more proton beam energy. We use a high-Z cone inserted into the capsule, driving the proton beam down a shielded path into the compressed fuel, which will slide along the cone wall. This scheme provides an efficient irradiation pattern and a relaxed short pulse laser focusing with a larger f/# focusing optics to provide a large stand-off distance of the optics from the reactor chamber. The cone has three additional advantages: (1) During injection of the capsule into the reactor chamber, the cone can serve as a heat shield against thermal radiation from the residual gas in the chamber, protecting the cryogenic fuel. (2) During the acceleration of the target for insertion into the reactor vessel, the cone acts as a contact for the inserter and sabot. (3) Use of a cone into a fuel pellet speeds up the fueling process with DT fusion fuel. The fuel can be applied in a drop of liquid fuel though the laser-drilled opening in the capsule where the cone will be inserted during fabrication and then closed by the cone and frozen together. A rapid

Fig. 7 Schematic illustration of the PFI approach of fast ignition with protons with a cone-in-shell target and proton acceleration from a curved foil inside the cone. First, the shell is compressed by a high-energy, nanosecond laser driver so that a dense fuel assembly is formed at the cone tip. Then, multiple ultra-intense short pulse laser beams generate the intense proton beam inside the cone from a curved foil. The protons stream through the cone tip into the dense DT fuel and release most of their energy in a small volume, which leads to ignition

1 Absorption and heat transport

2 Acceleration and rocket effect

3 Deceleration and compression

4 Laser-ion beam generation

5 Ion beam heating of dense fuel

6 Ignition and fusion burn
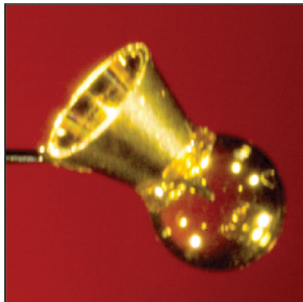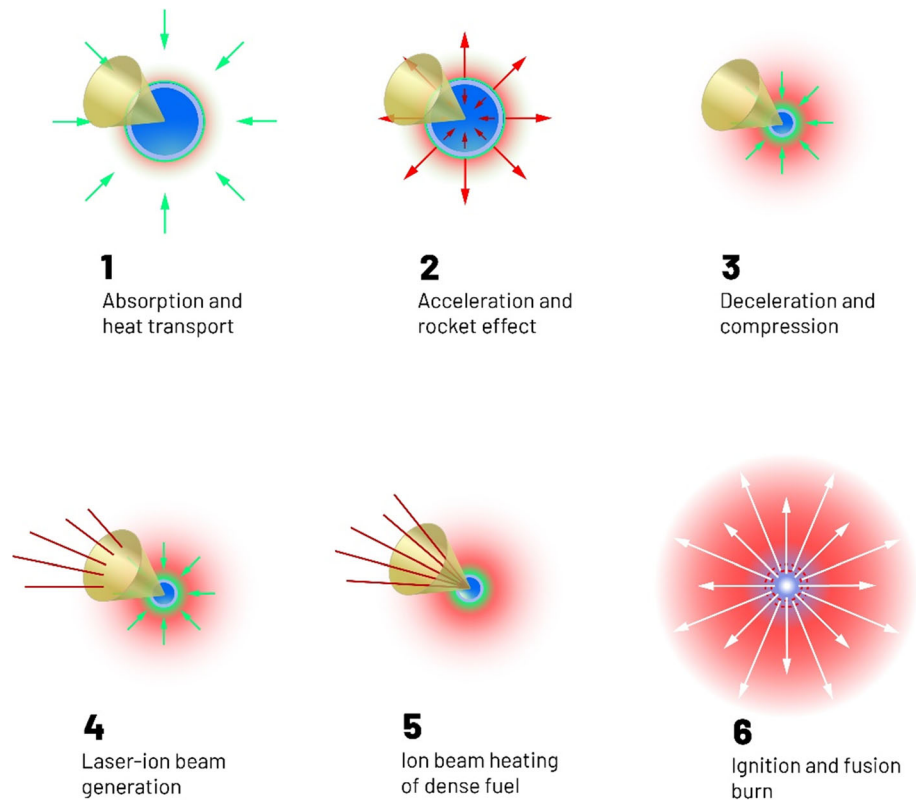
Fig. 8 Example of a cone-in-shell target used in integrated FI experiments on OMEGA. Figure reproduced from Ref. [45], American Institute of Physics

target filling scheme reduces the number of targets in process and the total inventory of tritium in the plant. An example picture of a fabricated cone-in-shell target (non-cryogenic) is depicted in Fig. 8 [45].

A summary of the decision process in choosing our IFE approach is illustrated by the flow chart diagram in Fig. 9. (1) The choice between indirect and direct drive compression is based on the difference in efficiency of compression. (2) The choice between direct central hot spot ignition and separating the ignition mechanism in a two-step process is motivated by the fact that lower implosion velocities are required, resulting in lower susceptibility to hydrodynamic instabilities and the fact that higher mass can be imploded leading to higher net yield. (3) The choice

of cone-in-shell geometry and a non-spherical implosion relaxes the high symmetry requirements of a spherical implosion. (4) Finally, protons are preferred over hot electrons for ignition as they can be focused to a smaller volume and better coupled to the dense fuel than electrons.

Current Understanding of the Underlying Physics of Proton Fast Ignition

Compression

The FE PFI approach requires compression to a density between 300 and 500 g/cm^3. That range of compression has been demonstrated experimentally at the NIF using 351 nm light [63]. We plan to use 2 ω (527 nm) light instead of the conventional 3 ω (351 nm) for the compression because it has considerable long-term benefits for a fusion power plant, in terms of lower facility costs and optics damage. However, most of the work that has been done on fuel compression and laser-plasma instabilities (LPI) is at 3 ω. Simple scaling relations imply that the ablation pressure scales as $P_{abl} \sim I_{abs}^{2/3} \lambda^{-2/3}$, where I_{abs} is the absorbed laser intensity and λ is the laser wavelength [64]. Assuming constant absorbed intensity, the simple model predicts that the ablation pressure is reduced by
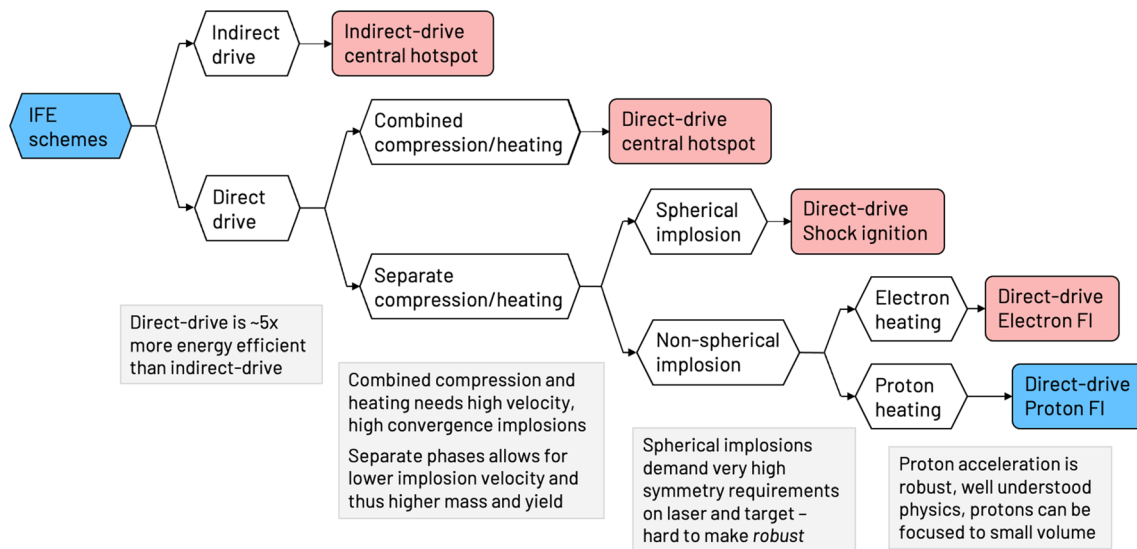
Fig. 9 The decision point flow chart which illustrates why Focused Energy has chosen proton fast ignition as its preferred approach to commercial IFE

$\sim 25\%$ when going from 3 to 2 ω. In addition, the absorbed intensity might be lower because of a decreasing efficiency in bremsstrahlung absorption. Detailed radiation hydrodynamic modeling will be performed at 3 ω and 2 ω to find the best tradeoff between physical risk and technical benefits. While the ablation pressure is reduced at 2ω, the increased stand-off distance of the critical surface from the ablation front (factor of ~ 7 longer for 2 ω than for 3 ω) may be beneficial for mitigating laser imprint.

There is also good experimental evidence that the non-spherical implosions needed in a cone-in-shell geometry are possible. For PFI, we do not have to coalesce all incoming shock waves at one point at the center and can employ thicker fuel layers than in hot spot ignition. Thus, the onset of hydrodynamic instabilities is less of a threat to achieving the correct fuel assembly compared to hot spot ignition. Experiments at OMEGA have shown good agreement between simulated and measured fuel assembly of a cone-in-shell target, giving confidence in the concept [65]. Figure 10 shows an experimental x-ray radiograph
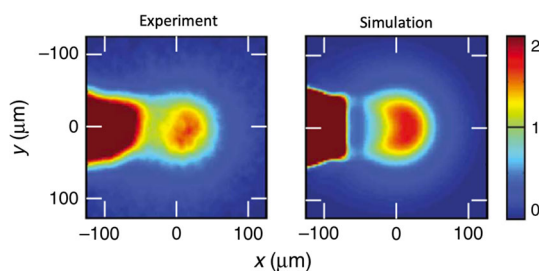
(left) of a cone-in-shell implosion on OMEGA at peak compression, which is in good agreement with the simulated radiograph (right).

Laser-Plasma Instabilities and Mitigation: 2 ω versus 3 ω Compression

In terms of the choice of wavelength for the compression pulses, the ICF community prefers the shortest wavelength as it improves the absorption of laser energy in the target [66–68] and it reduces laser plasma instabilities (LPI) [69, 70]. For this reason the Nd:glass ICF facilities such as NIF, Omega, and LMJ in France are all designed to operate at the 3rd harmonic of the 1053 nm fundamental of Nd:glass, a wavelength in the near UV at 351 nm. For similar reasons there are also proposals for use of KrF or ArF lasers operating further into the UV (e.g., 248 nm when KrF is employed) [65, 66].

These short wavelengths are not ideal for an actual commercial IFE plant. Optics are much more susceptible to optical damage at shorter wavelengths. Figure 11 shows the experimentally determined damage threshold for DKDP crystals (typically used for frequency doubling and tripling of Nd:glass lasers) as a function of wavelength for 10 ns duration pulses [71]. As it can be seen, 351 nm pulses damage at almost 1/3rd the fluence compared to 527 nm light. This is already a problem for single shot lasers such as NIF and it presents a severe problem in high repetition rate lasers needed for IFE. Therefore, we have decided that use of 527 nm light is desirable and perhaps even necessary for a successful commercial IFE scheme. This is FE's baseline approach for the compression lasers. Furthermore, use of 2 ω light allows the frequency
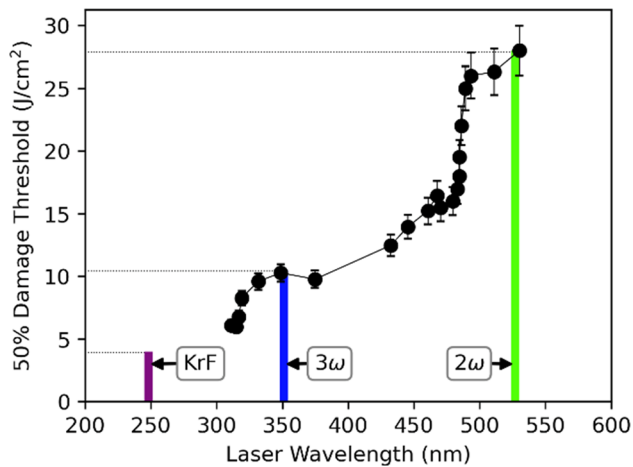

Fig. 10 Comparison of simulated and experimental x-ray radiograph of a compressed cone-in-shell target at the OMEGA laser. Figure reproduced from Ref. [63], Macmillan Publishers Limited

Fig. 11 Experimentally determined damage threshold for ~ 10 ns pulses on deuterated KDP crystals as a function of laser wavelength. Figure reproduced from Ref. 69. American Physical Society

conversion to be done back at the laser chain and the 527 nm can be transported with high damage threshold mirrors and lenses. This allows one to avoid having to put high value frequency conversion optics right at the reactor vessel wall (i.e., the target chamber) where neutron fluences might be high, which could lead to color center formation in the crystals.

The challenges that this choice poses are in reduced absorption efficiency and in the lower thresholds for the onset of deleterious LPI mechanisms that can significantly impact the implosion through reduced laser-target coupling, increased asymmetry, and hot electron preheat. The main concerns are Two Plasmon Decay (TPD) [67]. Stimulated Raman Scattering (SRS) [68]. Stimulated Brillouin Scattering (SBS) [15], and Cross Beam Energy Transfer (CBET) [72]. Recent theoretical studies have shown great progress in mitigating those instabilities [73, 74], opening the possibility to use 527 nm laser light. Our main strategy to suppress LPI is to use high-bandwidth pulses, which studies predict to be effective [73, 74]. We might also explore the use of spiked trains of uneven duration (STUD) pulses [75–77] and target solutions [78, 79] to mitigate LPI and to improve laser-target energy coupling. FE is currently performing 2ω LPI experiments on the European Light Infrastructure (ELI) L4 ATON laser [80, 81] and will use the green high-energy laser PHELIX for studying LPI mitigation techniques. Eventually, the effect of multi-beam LPI at 2ω will be studied in the future at FE's own facility. There is some good evidence, at least with 351 nm light, that the introduction of broad bandwidth onto the pulse increases the intensity threshold for the onset of LPI. The essence of the physics is that broad bandwidth decreases the coherence time in the laser pulse and inhibits coherent plasma wave formation.
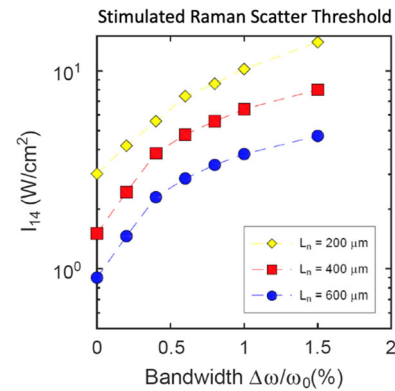

Fig. 12 Theoretically determined threshold for the onset of stimulated Raman scattering instability with 3ω light as a function of the laser bandwidth. Adapted from Ref. [72]

Figure 12 reproduces data from Ref. [72] plotting the intensity threshold for SRS onset as a function of bandwidth on the laser for three plasma density scale lengths. These data show a factor of 5 increase in the threshold intensity when 1.5% bandwidth is introduced. In the 1053 nm fundamental 1% bandwidth is 10 nm. This is challenging because of gain narrowing in the amplifiers of the laser but it can be achieved by use of very broadband front ends to inject pulses into the main amplifier chain. FE has developed a design for amplification of beamlines up to 7 kJ per beam at 2ω with 1% bandwidth.

Ignition

While separation of compression and heating in PFI has significant advantages in reducing laser drive energy and accessing high gain, it also poses challenges in generating the required particle beam to heat and ignite the compressed fuel. Detailed studies [82] have shown that these requirements can be met by a 20-kJ proton beam of radius 15–20 μm, with a particle distribution equivalent to a beam temperature of 4–8 MeV generated at most 1 mm away from the fuel. A conversion efficiency (CE) of 10–15% from a 150–200 kJ short pulse laser is required to deliver the necessary proton energy to the fuel within its disassembly time of 10–20 ps. Once the fuel is assembled the goal is to deliver a power density of $\sim 10^{22}$ W/cm^3 (~ 18 kJ in ~ 25 ps within a volume of linear dimension ~ 40 μm) to a compressed DT fuel at ~ 500 g/cm^3 with areal density of 2 g/cm^2. The energy must be delivered to the cold and dense part behind the cone tip. By curving the ion emitting target foil, ballistic focusing of ion beams down to a few 10 μm has been demonstrated [61]. The ion acceleration mechanism is known as the Target Normal Sheath Acceleration (TNSA) mechanism [49, 50] that has been extensively studied on many facilities over the last two decades. Several techniques have been found

to optimize laser-to-proton CE, including the use of mass-limited targets [53, 54, 83], heavy metal hydride coatings [51, 52], and laser pulse-shaping. The highest reported CE is 15% [84, 85]. Uncertainty remains in how CE will scale with more complex targets and an increase from experimentally studied drive laser energies of 10–1500 J to the required 150–200 kJ. Uncertainty also exists in the effect of overlapping multiple picosecond beams [42, 86].

Experiments have shown that the ions have the right energy spectrum needed for PFI and the conversion efficiency has reached a record of close to 15% from laser energy into useful ion beam energy, as illustrated in Fig. 13 [78]. A compilation of proton conversion efficiencies from many experiments as a function of laser energy is reproduced in Fig. 14 from Ref. [79]. These data suggest that at laser energy above a kJ, at least 10% energy efficiency into protons can be expected. This assertion drives the design for the short pulse lasers in an ignition machine and indicated that ~ 180 kJ is needed to get the necessary ~ 18 kJ into a hot spot.

As mentioned above, the proton pulse broadens in time as it propagates due to a spread in velocities, which is mitigated to some degree by the cone-guided approach to maintain the short pulse duration. In addition, as the most energetic ions penetrate the fuel, they start to heat up the fuel and the stopping power of the fuel to the lower energetic particle that arrive later decreases rapidly [87, 88]. Honrubia et al. predicted this range lengthening for the proton velocity range and DT plasma temperature range of interest for PFI, using the standard stopping power formula for classical plasmas [89]. One of the very few experimental results of proton stopping power in warm dense matter shows a decrease of the proton stopping power compared to that of cold solid matter [59]. The fortunate
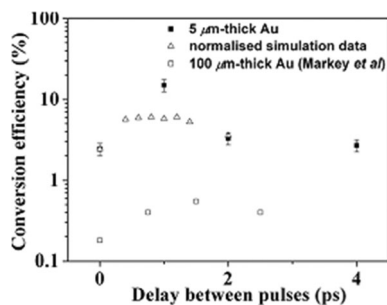

Fig. 14 Collection of various proton acceleration experiments plotting observed > MeV proton conversion efficiency as a function of laser energy. Figure reproduced from Ref. [79]. American Physical Society

result is that, using an appropriate velocity distribution, all ions tend to stop at the same depth, effectively adding up their kinetic energy in a narrow region.

Energy Production by IFE and Reactor Threat Spectrum

Inertial fusion energy (IFE) has several aspects which, from the standpoint of energy production are different than in magnetic fusion energy (MFE). Some are advantageous from the standpoint of ultimately constructing an energy-producing reactor. The released fusion energy is distributed among the fusion reaction products, which include charged particles, electromagnetic radiation, and neutrons. Each of the components takes part of the outgoing energy flux of the fusion fuel and must be dealt with to convert it efficiently into useable energy. The biggest difference between the two confinement schemes is that while MFE provides a steady stream of energy into the plasma facing wall material (first wall), in IFE the energy is delivered in short pulses, that cause a dynamic wall loading.

The released electromagnetic (EM) radiation is predominantly in the soft to mid x-ray region (photon energies of 1–50 keV), whose spectrum is determined by the temperature of the plasma. In addition, gamma radiation can be emitted from internal nuclear deexcitation processes after fusion events. While in MFE the radiation can cause embrittlement and sputtering of the first wall, the pulsed nature of the wall loading in IFE can also heat up the first few microns of the first wall to levels close to the melting point. All the EM radiation impinges onto the first wall within the lifetime of the fusion process (< ns). However, investigations have shown that wall material can be chosen to withstand this prompt flux [90].

Between 20 and nearly 100% of the fusion energy can be emitted as charged particles, dependent on the chosen

Fig. 13 Laser-to-proton energy conversion efficiency for protons with energy between 3.3 MeV and 35 MeV, useful for PFI, as a function of the delay between a picosecond pre-pulse and a high-intensity picosecond main pulse. The results were obtained for 5 μm-thick Au targets and are compared to results obtained with thicker (100 μm-thick) Au targets. Simulated laser-to-proton energy conversion efficiency (triangles) with respect to delay and normalized to the single pulse measured value is also shown. Figure reproduced from Ref. [78], American Institute of Physics
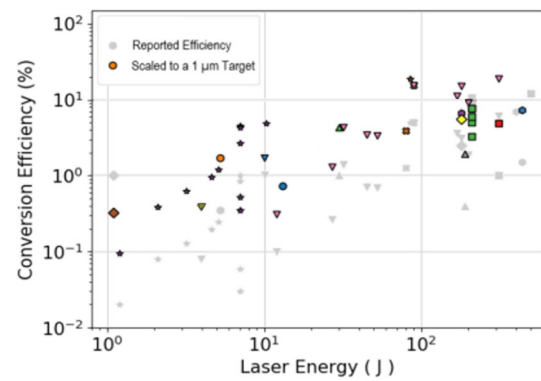
fuel type (of course with DT much of the energy is carried out by the 14 MeV neutrons). These charged particles also present a challenge to an IFE-based power plant. In contrast to the EM-radiation there is a flight dispersion of the charged particles, such that different energies and species arrive at different times on the reactor chamber wall [91]. The pulse lengthening relaxes the prompt wall loading on the first wall, but as most of the charged particles (mainly alpha particles) are stopped within a few micrometers, the energy deposition can reach temperatures which would cause the wall to start ablating for certain fuel types. The alpha particles will become He atoms inside the wall material and start to accumulate over time. This causes swelling and embrittlement of the wall material if not given the chance to find a free surface and diffuse out of the lattice. This pulsed nature of the EM and charged particle load on a reactor wall present different reactor vessel challenge than faced in MFE.

When DT fuel is employed up to 80% of the energy of the fusion process is emitted as neutrons. Neutrons can penetrate deep into the material, depending on their kinetic energy and will cause damage by displacing structural wall atoms from their original lattice position. Neutrons can also activate the reactor wall material. The latter is strongly dependent on the choice of the material. There are three main differences between the neutron wall loading and activation in MFE and IFE geometry. First, the materials to be used can be different in MFE and IFE. Whereas the close coupling of the functional components to the reactor vessel in MFE requires the specific materials that must be used (e.g., Niobium for super conducting-coils) the separation of the driver and the reactor in IFE allows for a much wider choice of low activating material.

The neutron spectrum is also slightly different in the two approaches [92]. In contrast to the thin, dilute plasma in MFE, with no influence on the neutron spectrum, in IFE the neutrons that are born with an energy of 14 MeV must travel some distance through the compressed fuel before reaching the free surface. As most of the neutrons are generated near the center of the pellet the collisions they experience as they leave the target softens the neutron spectrum. This is potentially helpful as a softened neutron spectrum has a different activation potential (e.g., in Si), thereby reducing the activation of the reactor.

Finally, there is a simple, but important geometrical effect as illustrated in Fig. 15. As a tokamak or stellarator gets larger for real energy production applications, the geometry of the neutrons born in the volume of the fuel start to resemble a 1D geometry, where a planar volume irradiates a wall. By contrast in IFE, if the target chamber is made larger there is a point like emitter facing the wall. The main difference is that in the IFE geometry the neutrons are typically at normal incidence to the wall, thereby maximizing the penetration depth. In MFE many neutrons are hitting the wall at a shallow angle. This causes the inner part of the wall to age much faster than in the IFE case. For this reason, we feel that IFE is very attractive and ultimately more likely to allow construction of a real reactor, a conclusion found in a number of studies on IFE concepts over the years [33, 85, 93].

With these reactor wall challenges in mind, the ultimate question for IFE commercialization is the gain and yield needed from the target. A very simple power cycle for a potential IFE plant is shown in Fig. 16. Essentially the fusion power output needed to drive a nominal 1 GW power plant, given inefficiencies of the thermal cycle and conversion to electricity is between 2.5 and 3 GW. With likely wall-plug efficiency of the drive lasers (frequency doubled laser energy out compared to electrical power in) of around 10%, one concludes that a fusion gain of around 100 (fusion energy out compared to drive laser energy in) is needed (coupled with the small additional gain achieved in a Lithium blanket which converts neutrons to Tritium). This mandates roughly a laser energy of 2.5 MJ per pulse operating at 10 Hz. This gain number and the yield are what drives our ultimate choice of approach to IFE commercialization.

Focused Energy Roadmap to Ignition Demonstration and an IFE Fusion Pilot Plant

As a conclusion to this discussion, we layout the roadmap that Focused Energy developed for IFE commercialization and describe the facilities that we think are needed to realize that roadmap. The goal of the plan is having a fusion pilot plant in the mid to late 2030s. This aggressive goal will demand R&D in four key areas and the development of test facilities along the way. Our principal R&D effort over the next 10 years is the design and construction of a laser facility that will demonstrate moderate to high gain by the PFI approach. We have named this facility Super-Nova and its planned specifications are listed below:
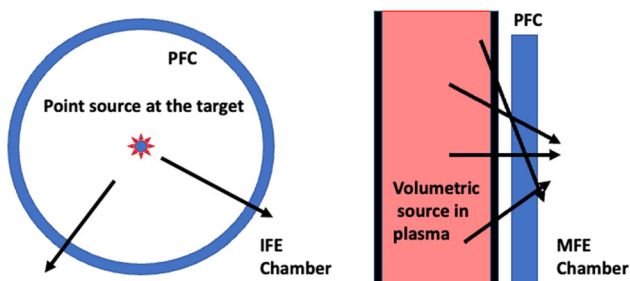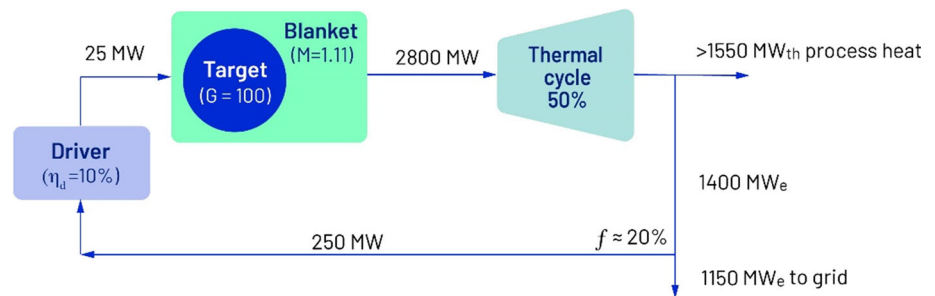

Fig. 15 Geometrical effect of neutron wall loading (NWL) on Plasma Facing Components (PFC) between IFE (left) and MFE (right)

Fig. 16 An example of the energy cycle and efficiencies that might be expected in an IFE-based power plant, illustrating why high gain of at least 100 is needed for commercial viability

- 100× long-pulse (nanosecond) beamlines, each delivering 5.5 kJ at 2 ω (527 nm)
- 550 kJ of total long-pulse energy at 2 ω
- 120× short-pulse (picosecond) beamlines, each delivering 1.5 kJ at 1 ω (1057 nm)
- 180 kJ of total short-pulse energy at 1 ω
- Shot rate of 1 shot every 3 min

The goal is to build this facility in the early 2030s to have a credible attempt at PFI ignition. This facility will have the advantage over existing single shot Nd:glass flashlamp pumped ICF facilities like the NIF and Omega, which fire at a rate of one shot every 45 min on OMEGA and one shot every few hours on NIF, that it will be designed to operate at greatly enhanced shot rate. Our current design is to operate full-energy shots every three minutes. This will be achieved by employing liquid cooled amplifier technology developed by National Energetics Inc, for the Extreme Light Infrastructure (ELI) Beamlines facility in Prague [78, 79]. Photos of these deployed 30 cm Nd:glass slab amplifiers are shown in Fig. 17. The basic concept is to cool the slabs by face cooling with flowing coolant. Multi-kJ operation of these amplifiers in the L4 beam line at a shot every 3 min has been demonstrated and utilized in experiments.

We have developed an evolution of this proven design for the multi-beam Super-Nova facility, in which 30 cm beam diameter amplifiers will be deployed in "quads" somewhat like the NIF beam architecture [94]. This design is illustrated in Fig. 18. The envisioned target chamber configuration for Super-Nova is illustrated in Fig. 19. The 100 long pulse beams for target compression will be frequency doubled and then transported to the target chamber, which is roughly 10 m in diameter. The 120 short-pulse beams with picosecond pulse duration will be first passed through pulse-compressor chambers (grey boxes) and then routed under the chamber for focusing into the target cone. The envisioned layout of the entire Super-Nova facility is illustrated in Fig. 20. This facility footprint is roughly half the size of the footprint of the NIF.
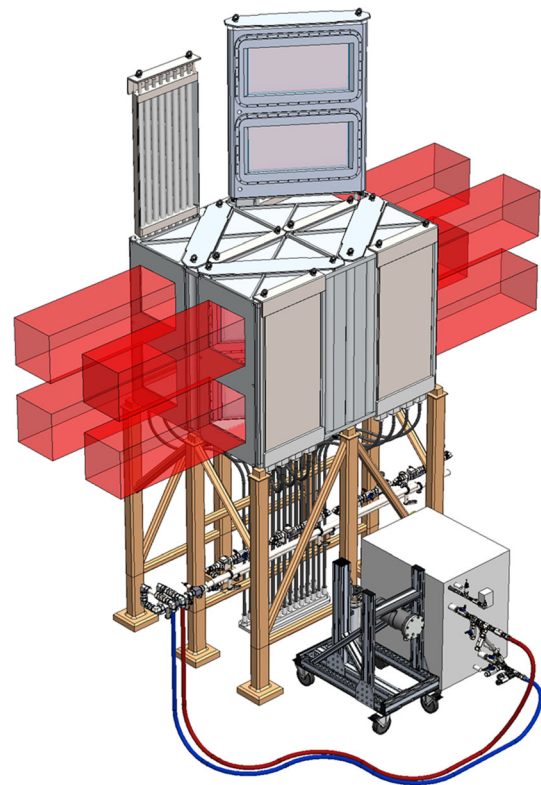

Fig. 17 Photo of liquid cooled 30 cm aperture Nd:glass slab amplifiers used for the ELI-Beamlines L4 ATON laser [78, 79]

Fig. 18 Engineering CAD drawing illustrating how the liquid cooled slab concept will be adapted to quad-beam configurations for the Super-Nova facility
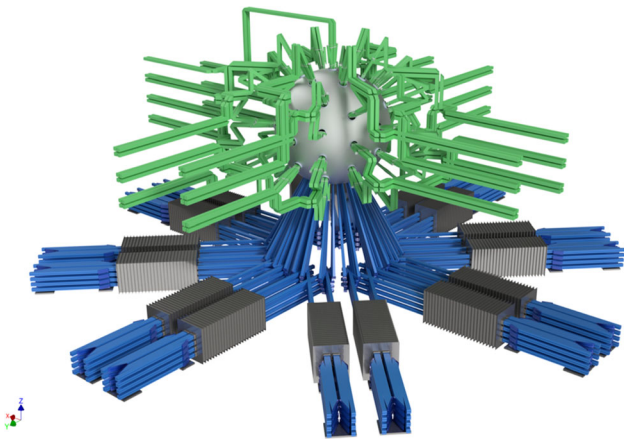
Fig. 19 CAD visualization of a potential ignition target chamber configuration for Super-Nova. The green beams symbolize the nanosecond compression laser beams, and the blue beams symbolize the short-pulse ignition beams that are routed through pulse compressors (gray boxes)

Prior to construction of Super-Nova, we will build a preliminary test facility, the Texas Science and Technology Advanced Research Laser or T-STAR. The layout of this facility is illustrated in Fig. 21. The first beamline of T-STAR will be a complete prototype beam for Super-Nova (in the spirit of the Beamlet laser as prototype beam for the

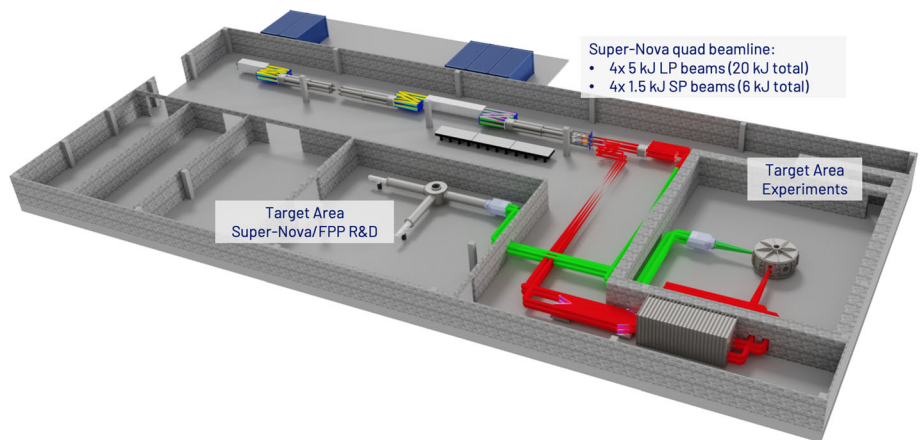**Fig. 20** Possible beam and target area configuration for Super Nova

NIF [95]. The roadmap plan is to then build out the laser to 8 beamlines (4 long pulse and 4 short pulse) to perform science de-risking experiments from 2028 onward, including 2 ω LPI experiments and proton acceleration efficiency optimization. Pulse parameter optimization will then serve to inform the final operational configuration of Super-Nova.

FE also will pursue three R&D efforts in parallel to Super-Nova: (1) Demonstrating a diode pumped solid state laser demonstrator at the 3-kJ level operating at 10 Hz and > 10% wall plug efficiency to serve as the prototype for the ultimate test power plant. (2) Development of the technique for manufacturing the 900,000 targets needed every day for an IFE power plant operation. (3) A reactor vessel design compatible with tritium breeding and 10 Hz power plant operation. These three efforts combined with demonstration of ignition will then feed into an ultimate fusion pilot plant (FPP) in the 2030s, which is named Quasar.

Conclusion

After many years of research, we have concluded that proton fast ignition (PFI) is the most credible approach for the commercialization of fusion energy within the inertial

Fig. 21 Visualization of the T-STAR prototype and de-risking facility

Super-Nova quad beamline:
- 4x 5 kJ LP beams (20 kJ total)
- 4x 1.5 kJ SP beams (6 kJ total)

Target Area
Super-Nova/FPP R&D

Target Area
Experiments

confinement fusion approach and that a PFI-based fusion power plant is indeed possible in the next two decades. Once the hot spot region has ignited and the bootstrapping alpha reactions have started driving a supersonic burn wave into the fuel, the yield of the pellet is only determined by the amount of assembled fuel mass and the areal density, which are only limited by the available drive laser energy of the long pulse compression beams. This approach might also pave the way to explore advanced fuels, by assembling targets where the burn wave can start propagating into other adjacent fuel compositions.

Declarations

References

1. J.D. Lawson, Some criteria for a power producing thermonuclear reactor. Proc. Phys. Soc. Lond. B **70**, 6 (1957)
2. "DOE National Laboratory Makes History by Achieving Fusion Ignition," https://www.energy.gov/articles/doe-national-laboratory-makes-history-achieving-fusion-ignition
3. J. P. Freidberg, Fusion energy and plasma physics, (Cambridge University Press, Cambridge, 2007).
4. J. Nuckolls, L. Wood, A. Thiessen, G. Zimmerman, Laser compression of matter to super-high densities: thermonuclear (ctr) applications. Nature **239**, 139–142 (1972)
5. S. Atzeni and J. Meyer-ter-vehn, The Physics of Inertial Fusion, (Clarendon, 2004).
6. J.D. Lindl, *Inertial confinement fusion: the quest for ignition and energy gain using indirect drive* (Springer-Verlag, New York, 1998)
7. E. Gibney, Nuclear-fusion reactor smashes energy record. Nature **602**, 371 (2022)
8. J. Mailloux et al., Overview of JET results for optimising ITER operation. Nucl. Fusion **62**, 042026 (2022)
9. M. Nocente, V. Kiptily, M. Tardocchi, P.J. Bonofiglo, T. Craciunescu, A. Dal Molin, E. De La Luna, J. Eriksson, J. Garcia, Z. Ghani et al., Fusion product measurements by nuclear diagnostics in the joint european torus deuterium–tritium 2 campaign (invited). Rev. Sci. Instrum. **93**, 093520 (2022)
10. H. Abu-Shawareb et al., Lawson criterion for ignition exceeded in an inertial fusion experiment. Phys. Rev. Lett. **129**, 075001 (2022)
11. R.S. Craxton, K.S. Anderson, T.R. Boehly, V.N. Goncharov, D.R. Harding, J.P. Knauer, R.L. McCrory, P.W. McKenty, D.D. Meyerhofer, J.F. Myatt et al., Direct-drive inertial confinement fusion: a review. Phys. Plasmas **22**(11), 110501 (2015)
12. E.M. Campbell, W.J. Hogan, The national ignition facilityapplications for inertial fusion energy and high-energy-density science. Plasma Phys. Control. Fusion **41**, B39 (1999)
13. E.I. Moses, Ignition on the national ignition facility. J. Phys. Conf. Ser. **112**, 012003 (2008)
14. T. Boehly, D.L. Brown, R.S. Craxton, R.L. Keck, J.P. Knauer, J.H. Kelly, T.J. Kessler, S.A. Kumpan, S.J. Loucks, S.A. Letzring et al., Initial performance results of the Omega laser system. Opt. Commun. **133**, 495 (1997)
15. D.A. Callahan, O.A. Hurricane, A.L. Kritcher, D.T. Casey, D.E. Hinkel, Y.P. Opachich, H.F. Robey, M.D. Rosen, J.S. Ross, M.S. Rubery, C.V. Young, A.B. Zylstra, A simple model to scope out parameter space for indirect drive designs on NIF. Phys. Plasmas **27**, 072704 (2020)
16. W. L. Kruer, *The physics of laser-plasma interactions*, Frontiers in Physics, Vol. 73, edited by D. Pines (Addison-Wesley, Redwood City, CA, 1988).
17. G.N. Hall, O.S. Jones, D.J. Strozzi, J.D. Moody, D. Turnbull, J. Ralph et al., The relationship between gas fill density and hohlraum drive performance at the national ignition facility. Phys. Plasmas **24**, 052706 (2017)
18. R. Betti et al., High-density and high ρr fuel assembly for fast ignition inertial confinement fusion. Phys. Plasmas **12**, 110702 (2005)
19. M. Roth, Review on the current status and prospects of fast ignition in fusion targets driven by intense, laser generated proton beams. Plasma Phys. Control. Fusion **51**, 014004 (2009)
20. O.A. Hurricane et al., Fuel gain exceeding unity in an inertially confined fusion implosion. Nature **506**, 343 (2014)
21. O.A. Hurricane, D.A. Callahan, D.T. Casey, E.L. Dewald, T.R. Dittrich, T. Döppner, S. Haan, D.E. Hinkel, L.F. Berzak Hopkins, O. Jones et al., Inertially confined fusion plasmas dominated by alpha-particle self-heating. Nat. Phys **12**, 800 (2016)
22. D.S. Montgomery, Two decades of progress in understanding and control of laser plasma instabilities in indirect drive inertial fusion. Phys. Plasmas **23**, 055601 (2016)
23. D.T. Casey, B.J. MacGowan, J.D. Sater, A.B. Zylstra, O.L. Landen, J. Milovich, O.A. Hurricane, A.L. Kritcher, M. Hohenberger, K. Baker et al., Evidence of three-dimensional asymmetries seeded by high-density carbon-ablator nonuniformity in experiments at the national ignition facility. Phys. Rev. Lett. **124**, 145002 (2020)

24. Lord Rayleigh, Investigation of the character of the equilibrium of an incompressible heavy fluid of variable density, in Scientific Papers (Cambridge University Press, Cambridge, England, 1900), Vol. II, pp. 200–207.

25. G. Taylor, The instability of liquid surfaces when accelerated in a direction perpendicular to their planes I. Proc. R. Soc. London Ser. A **201**, 192 (1950)

26. H. Takabe et al., Self-consistent growth rate of the Rayleigh-Taylor instability in an ablatively accelerating plasma. Phys. Fluids **28**, 3676 (1985)

27. J.D. Kilkenny, S.G. Glendinning, S.W. Haan, B.A. Hammel, J.D. Lindl, D. Munro, B.A. Remington, S.V. Weber, J.P. Knauer, C.P. Verdon, A review of the ablative stabilization of the Rayleigh-Taylor instability in regimes relevant to inertial confinement fusion. Phys. Plasmas **1**, 1379 (1994)

28. R. Betti, V.N. Goncharov, R.L. McCrory, C.P. Verdon, Growth rates of the ablative Rayleigh-Taylor instability in inertial confinement fusion. Phys. Plasmas **5**, 1446 (1998)

29. J.L. Milovich, H.F. Robey, D.S. Clark, K.L. Baker, D.T. Casey, C. Cerjan et al., Design of indirectly driven, high-compression inertial confinement fusion implosions with improved hydrodynamic stability using a 4-shock adiabat-shaped drive. Phys. Plasmas **22**, 122702 (2015)

30. O.L. Landen, J.D. Lindl, S.W. Haan, D.T. Casey, P.M. Celliers, D.N. Fittinghoff et al., Fuel convergence sensitivity in indirect drive implosions. Phys. Plasmas **28**, 042705 (2021)

31. V.N. Goncharov, T.C. Sangster, R. Betti, T.R. Boehly, M.J. Bonino, T.J.B. Collins et al., Improving the hot-spot pressure and demonstrating ignition hydrodynamic equivalence in cryogenic deuterium–tritium implosions on omega. Phys. Plasmas **21**, 056315 (2014)

32. T.J.B. Collins, C. Stoeckl, R. Epstein, W.A. Bittle, C.J. Forrest, V.Y. Glebov et al., Causes of fuel–ablator mix inferred from modeling of monochromatic time-gated radiography of omega cryogenic implosions. Phys. Plasmas **29**, 012702 (2022)

33. H.G. Rinderknecht, D.T. Casey, R. Hatarik, R.M. Bionta, B.J. MacGowan, P. Patel, O.L. Landen, E.P. Hartouni, O.A. Hurricane, Azimuthal drive asymmetry in inertial confinement fusion implosions on the national ignition facility. Phys. Rev. Lett. **124**, 145002 (2020)

34. O.M. Mannion, I.V. Igumenshchev, K.S. Anderson, R. Betti, E.M. Campbell, D. Cao, C.J. Forrest, M. Gatu Johnson, V.Y. Glebov, V.N. Goncharov et al., Mitigation of mode-one asymmetry in laserdirect-drive inertial confinement fusion implosions. Phys. Plasmas **28**, 042701 (2021)

35. M. Dunne, A high-power laser fusion facility for Europe, Nat. Phys. 2, 2 (2006), M. Dunne et al., "HIPER technical Background and conceptual design report," 2007.

36. HIPER project team, Preparatory Phase Study, Final Report, 2013.

37. M. Key et al.,Fast Ignition: physics progress in the US fusion energy program and prospects for achieving Ignition, Topic: OV/3–5, Research gate 2014.

38. W.R. Meier et al., Fusion technology aspects of laser inertial fusion energy (LIFE). Fusion Eng. Design **89**(9–10), 2489 (2014)

39. M. Tabak, J. Hammer, M.E. Glinsky, W.L. Kruer, S.C. Wilks, J. Woodworth, E.M. Campbell, M.D. Perry, R.J. Mason, Ignition and high gain with powerful lasers. Phys. Plasmas **1**, 1626 (1994)

40. R. Kodama, P.A. Norreys, K. Mima, A.E. Dangor, R.G. Evans, H. Fujita, Y. Kitagawa, K. Krushelnick, T. Miyakoshi, N. Miyanaga et al., Fast heating of ultrahigh-density plasma as a step towards laser fusion ignition. Nature **412**, 798 (2001)

41. R. Kodama, H. Shiraga, K. Shigemori, Y. Toyama, S. Fujioka, H. Azechi, H. Fujita, H. Habara, T. Hall, Y. Izawa et al., Nuclear fusion: fast heating scalable to laser fusion ignition. Nature **418**, 933 (2002)

42. R.B. Stephens, S.P. Hatchett, R.E. Turner, K.A. Tanaka, R. Kodama, Implosion of indirectly driven reentrant-cone shell target. Phys. Rev. Lett. **91**, 185001 (2003)

43. R. Betti, A.A. Solodov, J.A. Delettrez, C. Zhou, Gain curves for direct-drive fast ignition at densities around 300 g/cc. Phys. Plasmas **13**, 100703 (2006)

44. C. Stoeckl, T.R. Boehly, J.A. Delettrez, S.P. Hatchett, J.A. Frenje, VYu. Glebov, C.K. Li, J.E. Miller, R.D. Petrasso, F.H. Seguin et al., Hydrodynamics studies of direct-drive cone-in-shell, fast-ignitor targets on OMEGA. Phys. Plasmas **14**, 112702 (2007)

45. S. Atzeni, A. Schiavi, J.J. Honrubia, X. Ribeyre, G. Schurtz, Ph. Nicolai, M. Olazabal-Loume, C. Bellei, R.G. Evans, J.R. Davies, Fast ignitor target studies for the HiPER project. Phys. Plasmas **15**, 056311 (2008)

46. A.G. MacPhee, L. Divol, A.J. Kemp, K.U. Akli, F.N. Beg, C.D. Chen, H. Chen, D.S. Hey, R.J. Fedosejevs, R.R. Freeman et al., Limitation on prepulse level for cone-guided fast-ignition inertial confinement fusion. Phys. Rev. Lett. **104**, 055002 (2010)

47. W. Theobald, A.A. Solodov, C. Stoeckl, K.S. Anderson, R. Betti, T.R. Boehly, R.S. Craxton, J.A. Delettrez, C. Dorrer, J.A. Frenje et al., Initial cone-in-shell fast-ignition experiments on OMEGA. Phys. Plasmas **18**, 056305 (2011)

48. H.D. Shay, P. Amendt, D. Clark, D. Ho, M. Key, J. Koning, M. Marinak, D. Strozzi, M. Tabak, Implosion and burn of fast ignition capsules—Calculations with HYDRA. Phys. Plasmas **19**, 092706 (2012)

49. D.J. Strozzi, M. Tabak, D.J. Larson, L. Divol, A.J. Kemp, C. Bellei, M.M. Marinak, M.H. Key, Fast-ignition transport studies: realistic electron source, integrated particle-in-cell and hydrodynamic modeling, imposed magnetic fields. Phys. Plasmas **19**, 072711 (2012)

50. S. Atzeni, A. Schiavi, C. Bellei, Phys. Plasmas **14**, 052702 (2007)

51. R. Snavely et al., Intense high-energy proton beams from Petawatt-laser irradiation of solids. Phys. Rev Lett. **85**, 2945 (2000)

52. S.P. Hatchett, C.G. Brown, T.E. Cowan, E.A. Henry, J.S. Johnson, M.H. Key, J.A. Koch, A.B. Langdon, B.F. Lasinski, R.W. Lee et al., Electron, photon, and ion beams from the relativistic interaction of Petawatt laser pulses with solid targets. Phys. Plasmas **7**, 2076 (2000)

53. M.E. Foord, A.J. Mackinnon, P.K. Patel, A.G. MacPhee, Y. Ping, M. Tabak, R.P.J. Town, Enhanced proton production from hydride-coated foils. J. Appl. Phys. **103**, 056106 (2008)

54. D.T. Offermann, R.R. Freeman, L.D. Van Woerkom, M.E. Foord, D. Hey, M.H. Key et al., Observations of proton beam enhancement due to erbium hydride on gold foil targets. Phys. Plasmas **16**, 093113 (2009)

55. O. Tresca, D.C. Carroll, X.H. Yuan, B. Aurand, V. Bagnoud, C.M. Brenner et al., Controlling the properties of ultraintense laser–proton sources using transverse refluxing of hot electrons in shaped mass-limited targets. Plasma Phys. Control. Fusion **53**, 105008 (2011)

56. A. Morace, C. Bellei, T. Bartal, L. Willingale, J. Kim, A. Maksimchuk et al., Improved laser-to-proton conversion efficiency in isolated reduced mass targets. Appl. Phys. Lett. **103**, 054102 (2013)

57. C.M. Brenner, A.P.L. Robinson, K. Markey, R.H.H. Scott, R.J. Gray, M. Rosinski et al., High energy conversion efficiency in laser-proton acceleration by controlling laser-energy deposition onto thin foil targets. Appl. Phys. Lett. **104**, 081123 (2014)

58. A. Morace, N. Iwata, Y. Sentoku, K. Mima, Y. Arikawa, A. Yogo et al., Enhancing laser beam performance by interfering intense laser beamlets. Nat. Commun. **10**, 2995 (2019)

59. M. Roth et al., Fast Ignition by intense laser-accelerated proton beams. Phys. Rev. Lett. **86**, 436 (2001)

60. P.K. Patel, A.J. Mackinnon, M.H. Key, T.E. Cowan, M.E. Foord, M. Allen, D.F. Price, H. Ruhl, P.T. Springer, R. Stephens, Isochoric heating of solid-density matter with an ultrafast proton beam. Phys. Rev. Lett. **91**, 10–13 (2003)

61. T. Bartal, M.E. Foord, C. Bellei, M.H. Key, K.A. Flippo, S.A. Gaillard et al., Focusing of short-pulse high-intensity laser-accelerated proton beams. Nat. Phys. **8**, 139–142 (2012)

62. C. McGuffey, J. Kim, M.S. Wei, P.M. Nilson, S.N. Chen, J. Fuchs et al., Focusing protons from a kilojoule laser for intense beam heating using proximal target structures. Sci. Rep. **10**, 9415 (2020)

63. R. Tommasini, O.L. Landen, L. Berzak Hopkins, S.P. Hatchett, D.H. Kalantar, W.W. Hsing, D.A. Alessi, S.L. Ayers, S.D. Bhandarkar, M.W. Bowers et al., Time-resolved fuel density profiles of the stagnation phase of indirect-drive inertial confinement implosions. Phys. Rev Lett. **125**, 155003–155016 (2020)

64. W.M. Manheimer et al., Phys. Fluids. **25**, 1644 (1982)

65. W. Theobald, A.A. Solodov, C. Stoeckl, K.S. Anderson, F.N. Beg, R. Epstein et al., Time-resolved compression of a capsule with a cone to high density for fast-ignition laser fusion. Nat. Commun. **5**, 5785 (2014)

66. E. Fabre, F. Amiranoff, R. Fabbro, C. Garban-Labaune, J. Virmont, M. Weinfeld, F. David, and R. Pellat, *Effect of laser wavelength on interaction studies for inertial fusion*, in Plasma Physics and Controlled Nuclear Fusion Research 1980 (IAEA, Vienna, 1981), Vol. 2, pp. 263–272.

67. A.J. Schmitt, S.P. Obenschain, The importance of laser wavelength for driving inertial confinement fusion targets. I. Basic physics. Phys. Plasmas **30**, 012701 (2023)

68. A.J. Schmitt, S.P. Obenschain, The importance of laser wavelength for driving inertial confinement fusion targets. II. Target design. Phys. Plasmas **30**, 012702 (2023)

69. A. Simon, R.W. Short, E.A. Williams, T. Dewandre, On the inhomogeneous two-plasmon instability. Phys. Fluids **26**, 3107 (1983)

70. C.S. Liu, M.N. Rosenbluth, Parametric decay of electromagnetic waves into two plasmons and its consequences. Phys. Fluids **19**, 967 (1976)

71. C.W. Carr, H.B. Radousky, S.G. Demos, Wavelength dependence of laser-induced damage: determining the damage initiation mechanisms. Phys. Rev. Lett. **91**, 127402 (2003)

72. I. Igumenshchev, W. Seka, D. Edgell, D. Michel, D. Froula, V. Goncharov, R. Craxton, L. Divol, R. Epstein, R. Follett et al., Crossed-beam energy transfer in direct-drive implosions. Phys. Plasmas **19**, 056314 (2012)

73. J.W. Bates, J.F. Myatt, J.G. Shaw, R.K. Follett, J.L. Weaver, R.H. Lehmberg, S.P. Obenschain, Mitigation of cross-beam energy transfer in inertial-confinement-fusion plasmas with enhanced laser bandwidth. Phys. Rev. E **97**, 061202 (2018)

74. R.K. Follett, J.G. Shaw, J.F. Myatt, H. Wen, D.H. Froula, J.P. Palastro, Thresholds of absolute two-plasmon-decay and stimulated raman scattering instabilities driven by multiple broadband lasers. Phys. Plasmas **28**, 032103 (2021)

75. B. Afeyan, S. Hüller, Optimal control of laser plasma instabilities using spike trains of uneven duration and delay (STUD pulses) for ICF and IFE. EPJ. Web Conf. **59**, 05009 (2013)

76. S. Hüller, B. Afeyan, Simulations of drastically reduced sbs with laser pulses composed of a spike train of uneven duration and delay (STUD pulses). EPJ. Web Conf. **59**, 05010 (2013)

77. B.J. Albright, L. Yin, B. Afeyan, Control of stimulated raman scattering in the strongly nonlinear and kinetic regime using spike trains of uneven duration and delay. Phys. Rev. Lett. **113**, 045002 (2014)

78. A.A. Solodov, M.J. Rosenberg, M. Stoeckl, A.R. Christopherson, R. Betti, P.B. Radha, C. Stoeckl, M. Hohenberger, B. Bachmann, R. Epstein, R.K. Follett et al., Hot-electron preheat and mitigation in polar-direct-drive experiments at the national ignition facility. Phys. Rev. E **106**, 055204 (2022)

79. L. Ceurvorst, R. Betti, A. Casner, V. Gopalaswamy, A. Bose, S.X. Hu, E.M. Campbell, S.P. Regan, C.A. McCoy, M. Karasik, J. Peebles, M. Tabak, W. Theobald, Hybrid target design for imprint mitigation in direct-drive inertial confinement fusion. Phys. Rev. E **101**, 063207 (2020)

80. N. Jourdain, U. Chaulagain, M. Havlík, D. Kramer, D. Kumar, I. Majerová, V.T. Tikhonchuk, G. Korn, S. Weber, The L4n laser beamline of the P3-installation: towards high-repetition rate high-energy density physics at ELI-Beamlines. Matter Radiat. Extremes **6**, 015401 (2021)

81. F.P. Condamine et al., Commissioning results from the high-repetition rate nanosecond-kilojoule laser beamline at the extreme light infrastructure. Plasma Phys. Control. Fusion **65**, 015004 (2023)

82. S. Atzeni, M. Temporal, J.J. Honrubia, A first analysis of fast ignition of pre compressed ICF fuel by laser-accelerated protons. Nucl. Fusion **42**, L1–L4 (2002)

83. S. Buffechoux, J. Psikal, M. Nakatsutsumi, L. Romagnani, A. Andreev, K. Zeil et al., Hot Electrons Transverse Refluxing in Ultraintense Laser-Solid Interactions. Phys. Rev. Lett. **105**, 015005 (2010)

84. C. Brenner et al., High energy conversion efficiency in laser-proton acceleration by controlling laser-energy deposition onto thin foil targets. Appl. Phys. Lett. **104**, 081123 (2014)

85. M. Zimmer, S. Scheuren, T. Ebert, G. Schaumann, B. Schmitz, J. Hornung, V. Bagnoud, C. Rödel, M. Roth, Analysis of laser-proton acceleration experiments for development of empirical scaling laws. Phys. Rev. E **104**, 045210 (2021)

86. C.-K. Li, R.D. Petrasso, Charged-particle stopping powers in inertial confinement fusion plasmas. Phys. Rev. Lett. **70**, 3059 (1993)

87. L. Brown, D. Preston, R. Singleton Jr., Charged particle motion in a highly ionized plasma. Phys. Rep. **410**, 237–333 (2005)

88. J.J. Honrubia, M. Murakami, Ion beam requirements for fast ignition of inertial fusion targets. Phys. Plasmas **22**, 012703 (2015)

89. S. Malko, W. Cayzac, V. Ospina-Bohórquez, K. Bhutwala, M. Bailly-Grandvaux, C. McGuffey et al., Proton stopping measurements at low velocity in warm dense carbon. Nat. Commun. **13**, 2893 (2022)

90. J. Latkowski, K. Kramer, K. Abbott, K. Morris, J. DeMuth, L. Divol, B. El-Dasher, A. Lafuente, G. Loosmore, S. Reyes, et al., Integrated chamber design for the Laser Inertial Fusion Energy (LIFE) Engine, (2011).

91. J.M. Perlado et al., Design of HIPER IFE chambers for Engineering and Reactor facilities, ICENES, San Francisco (2011)

92. M. Sawan et al., Nuclear damage parameters for SiC/SiC composites in fusion systems Int. Symposium on SIC and Carbon-based materials for Fusion and Advanced Nuclear Energy Applications, Daytona Beach (2009).

93. E. Sistrunk, T. Spinka, A. Bayramian, S. Betts, R. Bopp, S. Buck, et al., All diode-pumped, high repetition- rate advanced petawatt laser system (HAPLS), Conference on Lasers and Electro-Optics, STh1L.2 (2017).

94. M.L. Spaeth, K.R. Manes, D.H. Kalantar, P.E. Miller, J.E. Heebner, E.S. Bliss, D.R. Spec, T.G. Parham, P.K. Whitman, P.J. Wegner et al., Description of the NIF Laser. Fusion Sci. Technol. **69**, 25 (2016)

95. B.M. Van Wonterghem, J.A. Caird, C.E. Barker, J.H. Campbell, J.R. Murray, D.R. Speck, Recent results of the national ignition facility beamlet demonstration project. Proc. SPIE **2633**, 22 (1995)